https://doi.org/10.36375/prepare_u.iei.a190

Post buckling analysis of silicon microneedle For publications of IEI

Ashok Kumar[1], Gnanavel BK[2] and Radhika C[1]

[1,2]Mechanical Department

([1]saveetha university, [2]Subject Matter Expert, L&T EduTech, Larsen and Toubro Construction)

([1]Saveetha nagar, Thandalam, Chennai-602105, [2]Mount Poonamallee Road, Manapakkam, Chennai - 600 089, INDIA)

{email: radhika@saveetha.ac.in}

Abstract – The microneedle is used to deliver the drug inside the skin structure. During the insertion procedure, the microneedle travel up to the dermis layer through the stratum corneum and epidermis layer. The microneedle have a tendency to critically buckle when the applied load achieves the maximum buckling load. To avoid structural failure of the microneedle, the critical load is identified and safely applied. In this paper, the critical buckling load is identified using the linear and non-linear buckling analysis. The critical load using linear buckling analysis is found to be 263.7µN. The non-linear or post -buckling analysis is performed for the load of 263.7µN and the critical load is found to be 149µN. Thus for silicon microneedle, the critical load is identified as 149µN. Henceforth for silicon microneedle, the applied load should always be smaller than the critical buckling load for safe insertion.

Keywords – Buckling analysis; microneedle; silicon; critical buckling load; finite element analysis; drug delivery.

INTRODUCTION

Microneedles play a vital role in delivering drugs into the human skin in an efficient way [1]. During the insertion process, the microneedle typically fails due to the bending and buckling effect [2] [3]. Among the buckling failure is considered as the foremost mode of failure of microneedle [4] [5]. The buckling analysis is proficient for finding the critical load experienced by the microneedle during the insertion process. Any load applied beyond the critical load will make the microneedle structurally fail. This infers that the load applied on the microneedle should not exceed the critical buckling load [6]. The buckling analysis is done using two approaches like linear and non-linear methods. Both methods help to determine the critical buckling load. Hence the load applied on the microneedle should always be lesser than the critical load calculated. This process of application will result in a safe insertion without structural failure.

A. Material selection

Microneedles are fabricated using various methods to attain different shapes, sizes, and material materials [7]. The occurrence of buckling on microneedles depends on the material and geometrical shape [8]. The shapes of the microneedle includes cylindrical, cone, pyramid, candle-like, tapered, bullet-shaped, spike and lancet [9], [10], [11], [12], [13], [14], [15], [16] . The appropriate selection of microneedle size and shape depends on the purpose of drug delivery into the human skin thereby resulting in a painless insertion [17]. The geometry with an aspect ratio of 12:1 length-diameter can result in a safe insertion without buckling [18]. In this paper, the conical shape is selected for analysis. The microneedle is modeled consisting of its height of 900µm, base diameter 600µm, and tip diameter as 60µm [19]. Microneedle is fabricated using various materials like silicon, glass, metal, composite, and polymer materials [20]. Each material has its advantage comparatively the conventional silicon material is easy to fabricate [21]. The silicon materials hold virtuous for micromachining and Micro electro-mechanical system (MEMS) application [22]. The only disadvantage of silicon material is it can easily break due to its brittle nature. This can be improved by applying load within the critical buckling limit. The young's modulus and ultimate strength of silicon microneedle is 110Gpa and 7000MPa [23].

B. Theoretical study

The critical buckling load for the polycarbonate microneedle is found to be 0.6N [6]. The buckling load measured on titanium

https://doi.org/10.36375/prepare_u.iei.a190

microneedle ranged from 0.5 to 1.2N [24]. The critical load is calculated by solving the following bending equation [25] as shown in equation (1). The parameters E, I(z), and M(z) represents the value of young's modulus of the material, the moment of inertia about the centroid, and bending moment distribution.

$$EI\,(z)\frac{d^2y(z)}{dz^2} + M(z) = 0 \quad (1)$$

Thereby solving the above bending equation, the critical buckling load for the hollow cone is given [26] as in equation (2). The parameters P_{cr}, L, d_0, d_i, and α represents critical buckling load, structural height, inner diameter, outer diameter, and tapering angle.

$$P_{cr} = \frac{E}{80\pi L^2} X \left[\frac{5\pi^2}{16}\left(d_0^4 - d_i^4\right) + \left(5\pi^2 + \frac{5}{4}\pi^4\right)\left(d_0^3 - d_i^3\right)\right] L\,tan\alpha + \left(15\pi^2 + \frac{5}{2}\pi^4\right)\left(d_0^2 - d_i^2\right)L^2\,tan\alpha^2 + \left(-120 + 30\pi^2 + \frac{5}{2}\pi^4\right)(d_0 - d_i)L^3\,tan\alpha^3] \quad (2)$$

C. Linear Buckling analysis

The linear buckling analysis is performed using the linear perturbation method using ABAQUS 6.14 software. The microneedle model is meshed using the C3D10 mesh element [27]. A unit load (1N) is applied on the top of the microneedle and the base is arrested. The mode shapes generated during the analysis is shown in Fig. 1, a) signifies the first mode shape experienced on the application of the load with eigenvalue 141.17, b) signifies the mode shape 2 with eigenvalue 143.81, c) signifies the mode shape 3 with eigenvalue 263.70, d) signifies the mode shape 4 with eigenvalue 267.77 and, e) signifies the final mode shape 5 with eigenvalue -271.17. Evaluating the different mode shapes, the microneedle buckled critically at mode shape 3 with eigenvalue 263.70. The eigenvalue of 263.70 is considered as the critical load applied on the microneedle. This infers the load applied on the microneedle should not exceed the buckling load of 263.70μN. The outcomes obtained during the linear buckling analysis of silicon microneedle are generated and represented in Table1. The eigenvalue, reaction force, displacement, and displacement rotation for the corresponding mode shape is listed.

TABLE I

(LINEAR BUCKLING ANALYSIS)

Mode No	Eigen value	Reaction force, N	Displacement mm	Displacement rotation, rad
0	0	0	0	0
1	141.17	179.214	1	1.634
2	143.81	147.346	1	1.636
3	263.7	96.298	1.182	263.7
4	267.77	499.238	1	1.316
5	271.17	466.718	1.013	0.002

D. Non-Linear buckling analysis

The post buckling analysis or non-linear buckling analysis is done using a static riks algorithm. The non-linear buckling analysis is done taking 263.7μN as input load or applied load. The boundary condition and constraints for the linear analysis are kept the same. The load proportionality factor (LPF) graph generated for silicon microneedle during the non-linear buckling analysis is shown in Fig. 2. The LPF steadily increases till it reaches the value of 0.4573 which refers to 45.73% of the applied load. From 45.73% of applied load, the structure experiences the buckling load. Once it reaches the value of 0.5646 i.e. 56.46% of applied load, the structure critically buckles leading to structural damage. The point where the structure experiences critical buckling behavior is considered as critical load. The critical buckling load, Pcr is calculated by means of the formulation as,

The Critical buckling load, Pcr = Load proportionality factor x Functional or Applied load.

Pcr = 0.5646*264

Pcr = 149μN

Critical buckling load, Pcr =149μN.

The critical load obtained on silicon microneedle is observed as 149μN. Thus, for the non-linear buckling analysis, the critical load is identified as 149μN.

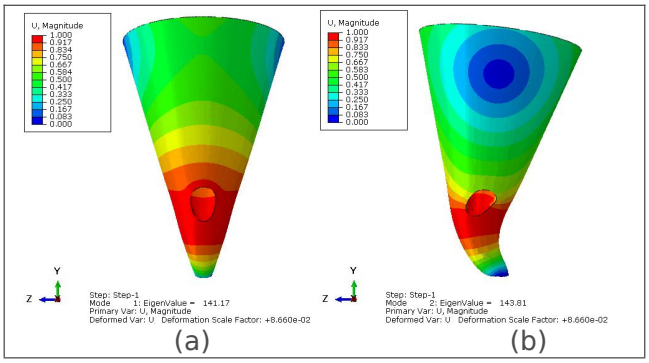

(a) (b)

https://doi.org/10.36375/prepare_u.iei.a190

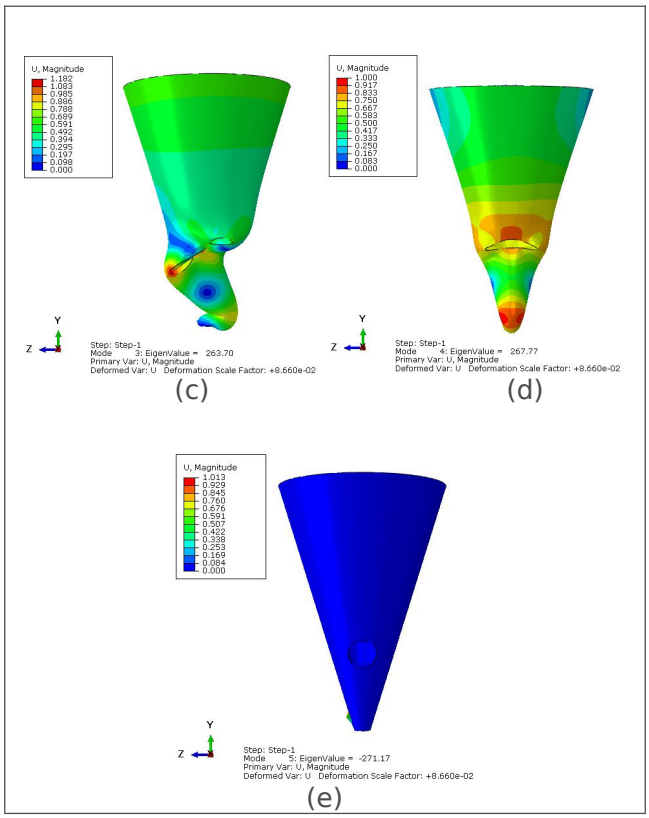

Fig. 1 Linear buckling analysis of silicon microneedle with different mode shapes.

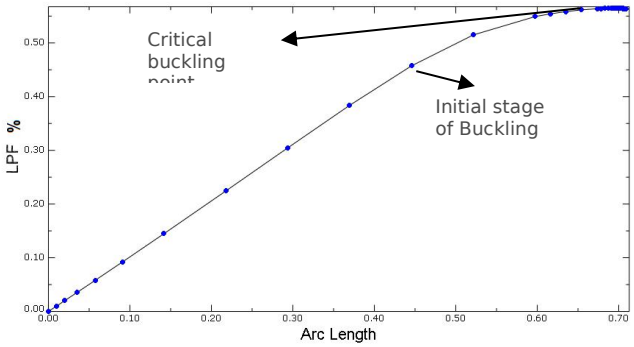

Fig. 2 The load proportionality graph exerted for silicon microneedle

CONCLUSION

The process of buckling analysis is to identify the critical buckling load acting on the microneedle during the insertion process. The silicon conical-shaped microneedle is selected for performing the analysis. The buckling analysis is executed in two ways consisting of linear and non-linear or post-buckling method. The critical buckling load during the linear and non-linear approach is found to be 263.7μN and 149μN. This infers that the microneedle critically buckles and fails if the applied load is beyond the 149μN. thereby applying loads within the critical limit will prevent the microneedle from failure and thus result in a safe insertion. This process holds good for calculating the insertion force of the microneedle.

NOMENCLATURE

C3D10	10-node quadratic tetrahedron element
d_i	inner diameter
d_0	outer diameter
E	young's modulus of the material
I(z)	moment of inertia about the centroid
L	structural height
LPF	load proportionality factor
M(z)	bending moment distribution
Pcr	Critical buckling load
μN	micro newton
α	tapering angle

ACKNOWLEDGMENT

The author would like to thank our institution Saveetha University for their support and guidance throughout the research work.

REFERENCES

[1] V. R. Manoj and H. Manoj, "Review on Transdermal Microneedle-Based Drug Delivery," *Asian J. Pharm. Clin. Res.*, vol. 12, no. 1, p. 18, 2019.

[2] M. W. Ashraf *et al.*, "Design, fabrication and analysis of silicon hollow microneedles for transdermal drug delivery system for treatment of hemodynamic dysfunctions," *Cardiovasc. Eng.*, vol. 10, no. 3, pp. 91–108, 2010.

[3] D. W. Bodhale, A. Nisar, and N. Afzulpurkar, "Design , Fabrication and Analysis of Silicon Microneedles for Transdermal Drug Delivery Applications Design , fabrication and analysis of silicon microneedles for transdermal drug delivery applications," *Proc. 3rd Int. Conf. Dev. BME Vietnam*, no. January, 2010.

[4] E. Z. Loizidou *et al.*, "Structural characterisation and transdermal delivery studies on sugar microneedles: Experimental and finite element modelling analyses," *Eur. J. Pharm. Biopharm.*, vol. 89, pp. 224–231, 2015.

[5] M. A. Kosoglu, R. L. Hood, and C. G. Rylander, "Mechanical strengthening of fiberoptic microneedles using an elastomeric support," *Lasers Surg. Med.*, vol. 44, no. 5, pp. 421–428, 2012.

[6] C. Radhika and B. K. Gnanavel, "Buckling analysis of polymer microneedle for transdermal drug delivery," *Mater. Today Proc.*, vol. 46, no. September, pp. 3538–3541, 2020.

[7] M. R. Prausnitz, "Microneedles for transdermal drug delivery," *Adv. Drug Deliv. Rev.*, vol. 56, no. 5, pp. 581–587, 2004.

[8] Z. F. Rad *et al.*, "High-fidelity replication of thermoplastic microneedles with open microfluidic channels," *Microsystems Nanoeng.*, vol. 3, no. April, pp. 1–11, 2017.

[9] B. Chua, S. P. Desai, M. J. Tierney, J. A. Tamada, and A. N. Jina, "Effect of microneedles shape on skin penetration and minimally invasive continuous

glucose monitoring in vivo," *Sensors Actuators, A Phys.*, vol. 203, pp. 373–381, 2013.
[10] K. Lee, C. Y. Lee, and H. Jung, "Dissolving microneedles for transdermal drug administration prepared by stepwise controlled drawing of maltose," *Biomaterials*, 2011.
[11] J. Ji, F. E. H. Tay, J. Miao, and C. Iliescu, "Microfabricated microneedle with porous tip for drug delivery," *J. Micromechanics Microengineering*, vol. 16, no. 5, pp. 958–964, 2006.
[12] Jung-Hwan Park, Yong-Kyu Yoon, M. R. Prausnitz, and M. G. Allen, "High-aspect-ratio tapered structures using an integrated lens technique," *IEEE*, pp. 383–386, 2004.
[13] M. Shikida *et al.*, "Non-photolithographic pattern transfer for fabricating arrayed three-dimensional microstructures by chemical anisotropic etching," *Sensors Actuators, A Phys.*, vol. 116, no. 2, pp. 264–271, 2004.
[14] K. Y. Seong *et al.*, "A self-adherent, bullet-shaped microneedle patch for controlled transdermal delivery of insulin," *J. Control. Release*, vol. 265, no. October 2016, pp. 48–56, 2017.
[15] P. Griss and G. Stemme, "Novel, side opened out-of-plane microneedles for microfluidic transdermal interfacing," *Tech. Dig. MEMS 2002 IEEE Int. Conf. Fifteenth IEEE Int. Conf. Micro Electro Mech. Syst. (Cat. No.02CH37266)*, pp. 467–470, 2002.
[16] P. Dardano, A. Caliò, V. Di Palma, M. F. Bevilacqua, A. D. Di Matteo, and L. Stefano, "A photolithographic approach to polymeric microneedles array fabrication," *Materials (Basel).*, vol. 8, no. 12, pp. 8661–8673, 2015.
[17] B. Stoeber and D. Liepmann, "Arrays of Hollow out-of-Plane Microneedles for Drug Delivery," *JMEMS 1243*, 2004.
[18] J.-H. Park and M. R. Prausnitz, "Analysis of Mechanical Failure of Polymer Microneedles by Axial Force," *J Korean Phys Soc.*, vol. 56, no. 4, pp. 1223–1227, 2011.
[19] M. S. ausse Lhernould, M. Deleers, and A. Delchambre, "Hollow polymer microneedles array resistance and insertion tests," *Int. J. Pharm.*, vol. 480, no. 1–2, pp. 152–157, 2015.
[20] N. Wilke, A. Mulcahy, S. R. Ye, and A. Morrissey, "Process optimization and characterization of silicon microneedles fabricated by wet etch technology," *Microelectronics J.*, vol. 36, no. 7, pp. 650–656, 2005.
[21] M. N. Abser, "Solid Silicon Microneedles for Safe and Effective Drug Delivery to Human Eye," 2009.
[22] N. Mane and A. Gaikwad, "Design , Simulation and Analysis of Micro needle for Drug Delivery using Structural and Fluid Flow Mechanics," *Int. J. Mech. Prod. Eng.*, vol. 2, no. 1, pp. 5–8, 2013.
[23] E. Larrañeta, R. E. M. Lutton, A. D. Woolfson, and R. F. Donnelly, "Microneedle arrays as transdermal and intradermal drug delivery systems: Materials science, manufacture and commercial development," *Mater. Sci. Eng. R Reports*, vol. 104, pp. 1–32, 2016.
[24] E. R. Parker, M. P. Rao, K. L. Turner, C. D. Meinhart, and N. C. MacDonald, "Bulk micromachined titanium microneedles," *J. Microelectromechanical Syst.*, 2007.
[25] Smith Garth W, "Analytic solutions for tapered column buckling," *Compufers It Slrucfures*, vol. 28, no. 5, pp. 677–681, 1988.
[26] K. Kim *et al.*, "A tapered hollow metallic microneedle array using backside exposure of SU-8," *J. Micromechanics Microengineering*, 2004.
[27] C. Radhika and B. K. Gnanavel, "Finite element analysis of polymer microneedle for transdermal drug delivery," *Mater. Today Proc.*, vol. 39, no. 4, pp. 1538–1542, 2020.